# MELTING CHARACTERISTICS OF CAPSULATED PHASE CHANGE MATERIALS

*Ahmad A. Sultan [a], Emad Al-Negiry [a], Ali Radwan [a], Mohammad Alawady [b]*

*[a] Mansoura University, Faculty of Engineering, Mechanical Power Department, Egypt*
*[b] Al-Diwaniyah Governorate, Al- Diwaniyah Water Directorate, Iraq*

**ABSTRACT**:

An experimental and computational investigation studied phase change material melting in a cylindrical capsule with PCM. The capsule is placed horizontally in a rectangular test section, where it is insulated from all sides' wall except the front one. The PCM capsule is heated by passing hot water from downward to upward with different inlet mean water temperatures (327.9, 333.7, 338 and 343) K, different velocities, varied thermal conductivities of capsule material wall (copper, iron, pyrex-glass, and polyethylene), and PCM. Experiment during melting inside a pyrex-glass capsule was performed and compared with prediction analysis by using CFD ANSYS 2019 R2. Image processing of melting photographs along with melted time were used in comparison. The comparison between the liquid fraction and energy stored with time for lauric acid and paraffin wax was analyzed. PCM liquid fraction, temperature and energy stored measurements for lauric acid were assessed numerically. The results reveal for lauric acid that the total melting time was enhanced 43% for 4.6% increase in water mean inlet temperature, 18% for 500% increase in inlet water mean velocity, and 7% when used copper capsule wall. The results proved that the lauric acid charged with energy stored were 47% more than paraffin wax during the total melting time of it, and the effect of different water mean inlet temperatures was the main factor for the charging process to improve the PCM melting time.

**ملخص البحث:**

دراسة عملية ونظرية لانصهار مادة متغيرة الطور في كبسولة أسطوانية. توضع الكبسولة أفقياً في مقطع اختبار مستطيل ، حيث يتم عزله من جميع الجوانب باستثناء الجزء الأمامي. يتم تسخين الكبسولة عن طريق تمرير الماء الساخن من الأسفل إلى الأعلى بدرجات حرارة مختلفة (٣٢٧.٩ ، ٣٣٣.٧ ، ٣٣٨ و ٣٤٣) K ، سرعات مختلفة ، معامل توصيل حراري متنوع لمادة جدار الكبسولة (النحاس ، الحديد ، زجاج البيركس ، و البولي ايثيلين) ، تم إجراء تجربة أثناء الانصهار داخل كبسولة من -زجاج البيركس ومقارنتها بالنتائج النظرية باستخدام CFD ANSYS 2019 R2 . تم تسجيل النتائج النظرية لنسبة لحامض اللوريك المنصهر ، ودرجة حرارته المتوسطة والطاقة المخزنة به. أوضحت النتائج لحامض اللوريك أن زمن الانصهار الكلي قد تحسن بنسبة ٤٣٪ بزيادة قدرها 4.6٪ في متوسط درجة حرارة الماء الداخل ، و ١٨٪ بزيادة ٥٠٠٪ في متوسط سرعة الماء الداخل ، و ٧٪ عند استخدام جدار كبسولة من النحاس. أثبتت النتائج أن الطاقة المخزنة في حمض اللوريك تزيد بنسبة ٤٧٪ عن شمع البارافين خلال فترة الانصهار الكلية للبرافين .

*Keywords*: (Melting process, Lauric Acid, PCM capsule, Horizontal cylinder, Numerical)

| Nomenclature | | Greek symbols | |
|---|---|---|---|
| $A_{mush}$ | mushy zone constant | $\beta$ | thermal expansion coefficient (1/K) |
| $C_p$ | specific heat capacity (J/K kg) | $\lambda$ | liquid fraction |
| $F_B$ | buoyancy force | $\mu$ | dynamic viscosity (Pa. s) |
| $g$ | gravity (m/s$^2$) | $\rho_l$ | liquid density (kg/m$^3$) |
| $H$ | enthalpy (J/kg) | $\rho_s$ | solid density (kg/m$^3$) |
| $h$ | sensible enthalpy (J/kg) | | |
| $h_{ref}$ | reference enthalpy (J/kg) | Abbreviations | |
| $k$ | thermal conductivity (W/K m) | CFD | computational fluid dynamics |
| $L$ | latent heat of melting (J/kg) | CPVC | chlorinated polyvinyl chloride |
| $S$ | momentum source term (pa/m) | EPCMs | encapsulated phase change |
| $T$ | temperature (K) | | |
| $t$ | time (s) | materials | |
| $T_s$ | solidus temperature (K) | HTF | heat transfer fluid |
| $T_{initial}$ | initial temperature (K) | PCM | phase change material |
| $T_l$ | liquidus temperature (K) | PDEs | partial differential equations |
| $T_m$ | melting temperature (K) | PRESTO | pressure staggering option |
| $u$ | velocity (m/s) | SIMPLE | semi-implicit scheme |
| | | TES | thermal energy storage |

# 1. INTRODUCTION

Increasing continuously of the consumption demands of energy in transport field, industrial sectors, and domestic make the solar energy as a renewable and sustainable clean source and the energy that can fulfill the requirements. The main drawbacks and the problem of discontinuity can be solved by storing the energy. Higher heat transfer (charging and discharging cycles) during the melting or solidification of a phase change materials (PCMs) became more attractive in the recent decades due to its relevance to many technological applications especially in thermal storage systems. Several experimental and mathematical models were developed to provide the basis for an optimum design of the latent heat storage unit LHSU, [1].

[2] examined the storage capabilities and potential for storage deterioration in cylindrical capsules to determine the types of encapsulated phase change materials (EPCMs) suitable for thermal energy storage (TES) system. Several kinds of PCMs were considered for the experiments and simulations, including metals like zinc and aluminum; salts like NaNO$_3$, NaCl-MgCl$_2$ eutectic (57% mole fraction NaCl and 43% mole fraction MgCl$_2$), MgCl$_2$, and NaCl. Stainless steel 304 (chromium and nickel) or carbon steel was selected as the encapsulation shell with around 1.5875 mm (1/16 inch) thickness.

[3] investigated the role of natural convection on solid-liquid interface motion during constrained melting within a horizontal cylindrical Gallium capsule. A numerical code was developed using an unstructured finite-volume method, an enthalpy porosity technique. It was found that the melting process of PCM was dominated by conduction at early stages indicated by concentric solid–liquid interfaces parallel to the circular heated wall. At later times, natural convection was augmented and this affected the shape of the melting front and consequently results in unsymmetrical melting about the horizontal axis of the capsule.

[4] numerically analyzed the melting process around a horizontal circular Gallium cylinder in the presence of the natural convection in the melt phase. Two boundary conditions were investigated one of constant wall temperature over the surface of the cylinder and the other of constant heat flux. It is found that, independent of the boundary condition, melting of PCM in the bottom part is very inefficient because the energy charged to the system is mainly transferred to the upper part of the cylinder by the convective flow in the melt.

[5] numerically studied the thermal energy storage using capsulated cylinders filled with PCM. These cylinders were arranged in-line in the direction of heat transfer fluid. The results showed that the increment of both Reynolds number and the ratio of the pitch (l) (longitudinal pitch is equal to transverse pitch) to diameter (l/D) gave decrement in the final time of melting of PCM in the cylinders.

[6] experimentally and computationally investigation reported for understanding the role of buoyancy-driven convection during constrained melting of phase change materials (PCM) inside a spherical capsule. Paraffin wax n-octadecane was constrained during melting inside a transparent glass sphere through the use of thermocouples installed inside the sphere.

[7] presented a comparative study of three different mathematical models for the packed bed latent heat storage system, comprised of a cylindrical storage tank filled with paraffin encapsulated plastic spherical containers which were packed randomly inside the tank. The results obtained by solving the models using the fully explicit finite difference method were initially validated with experimental results. Further numerical analysis was performed using the models for two different heat transfer fluids of air and water at different mass flow rates and ball sizes and the validity of the models were compared and reported. It was found that one model was sufficient when air was the heat transfer fluid and another model was recommended when water was the heat transfer fluid.

[8] analyzed numerically a two dimensional sphere model with hallow section as a test section. The melting behavior of PCM was predicted using the finite volume based CFD tool ANSYS Fluent. The diameter of hollow section of sphere was 84 mm. The aluminum wall thickness was 1 mm. The isothermal boundary condition was taken for numerical simulation. The Paraffin wax, Sodium acetate tri-hydrate and Lauric acid were tested for energy storage and for performance analysis. The melted PCMs were collected at top of 2D sphere due to natural convection and gravity effect. The rate of melting in Sodium acetate tri-hydrate was more compared to Lauric acid, Paraffin wax due to its thermal properties. Thus at given time energy storage capacity was more in Sodium acetate tri-hydrate.

[9] numerically and experimentally analyzed a 3D axisymmetric model of the heat transfer during the melting process of a PCM inside a spherical container. The mathematical model was solved using the "Volume of Fluid Method," and the "Enthalpy-Porosity Formulation" was employed to solve the energy equations in both the liquid and solid regions of the PCM, using the Fluent software. It was found that at a constant value of Stefan Number, increasing the Grashof Number would enhanced the heat transfer rate. Additionally, the combined effect of the Grashof and Stefan Numbers at an increase of the outer surface temperature of the enclosure could also enhanced the melting rate of the PCM. [10] numerically studied a packed bed heat storage system using spherical capsules filled with three kinds of PCM. The capsules are filled into a packed bed which is connected with a flat plate solar collector. The capsules are placed in series based on the melting temperature of PCM. Water is used as heat transfer fluid (HTF) and heated in the solar collector. The comparison results indicate that this new type heat storage packed bed has higher energy and exergy transfer efficiencies than the traditional packed bed, and the average energy and exergy collection efficiency of its solar collector are higher too.

The present work focuses on low melting temperature encapsulated phase change materials for thermal energy storage (TES) system. The objectives of the present experimental and numerical work are:

(i) To develop and compare a numerical model for CFD analysis of capsulated PCMs in a two dimensional horizontal cylinder by using Ansys Fluent 2019 R2 and to solve for natural convection coupled to solid-liquid phase change.

(ii) To investigate numerically the natural convection dominated melting of a PCM within a horizontal cylindrical capsule and estimate the melt fraction and temperature contours.

(iii) To compare the energy stored at a given time of simulation. The above objectives will be studied at different HTF inlet temperatures, different velocities of heat transfer fluid (HTF), different material types of capsulated shell (copper, iron, pyrex-glass, and polyethylene), and different PCM type.

## 2. NUMERICAL MODEL
### 2.1. Governing equations

In the present study, the combined convection-diffusion phase transition of the PCM is modeled applying the enthalpy-porosity formulation. In this method, the PCM is treated as a "pseudo" porous zone, in which the porosity is defined by the value of liquid fraction ($\lambda$) which varies between 0 and 1, where the 0 represents a solid zone while 1 represents a liquid zone. The liquid PCM is assumed to be Newtonian, two-dimensional, incompressible, and unsteady flow. Moreover, the liquid PCM density variation in buoyancy force term is modeled by the Boussinesq approximation in order to involve thermal buoyancy which gives rise to natural convection. The 2D phase transition process (governing equations) analysis of PCM during melting, including buoyancy driven

convection in the molten PCM can be written as follows [11] and [12];

Continuity equation:
$$\frac{\partial u}{\partial x} + \frac{\partial v}{\partial y} = 0 \qquad \dots (1)$$

Momentum equation (in x- direction):
$$\rho \frac{\partial u}{\partial t} + \rho u \frac{\partial u}{\partial x} + \rho v \frac{\partial u}{\partial y} = -\frac{\partial P}{\partial x} + \mu \left(\frac{\partial^2 u}{\partial x^2} + \frac{\partial^2 u}{\partial y^2}\right) + S_x \quad .. (2)$$

Momentum equation (in y- direction):

$$\rho \frac{\partial v}{\partial t} + \rho u \frac{\partial v}{\partial x} + \rho v \frac{\partial v}{\partial y} = -\frac{\partial P}{\partial y} + \mu \left(\frac{\partial^2 v}{\partial x^2} + \frac{\partial^2 v}{\partial y^2}\right) + F_B + S_y \qquad \dots (3)$$

Where $\rho$ is the density (kg/m$^3$); u, v are the velocities of the PCM liquid phase (m/s) in x and y directions, respectively, P is the pressure (Pa); $\mu$ is the dynamic viscosity (Pa s); $F_B$ is a buoyancy force given by the Boussinesq approximation
$$F_B = -\rho_o \left(1 - \beta_1 (T - T_o)\right) g \qquad \dots (4)$$

The terms $\rho_o$, $\beta_1$, $T_o$ and g are the operating density (density of the liquid PCM ($\rho_o = \rho_l$ (kg/m$^3$)), the thermal expansion coefficient (1/K), the operating temperature ($T_o = T_m$ (°C)), and the gravitational acceleration (m/s$^2$), respectively. The parameters $S_x$, and $S_y$ are Darcy's law damping terms (source term) or the porosity function that are added to the momentum equations due to the phase change effect on convection.

Energy equation for liquid phase:
$$\rho_l \frac{\partial H}{\partial t} + \rho_l u \frac{\partial H}{\partial x} + \rho_l v \frac{\partial H}{\partial y} = k_l \left(\frac{\partial^2 T}{\partial x^2} + \frac{\partial^2 T}{\partial y^2}\right) \quad \dots (5)$$

Energy equation for solid phase:
$$\rho_s \frac{\partial H}{\partial t} = k_s \left(\frac{\partial^2 T}{\partial x^2} + \frac{\partial^2 T}{\partial y^2}\right) \qquad \dots (6)$$

where H is the enthalpy of the material (J/kg), and is computed as the sum of the sensible enthalpy, $h_1$, and the latent heat, $\Delta H$:
$$H = h_1 + \Delta H \qquad (J/kg) \qquad \dots (7)$$
$$h_1 = h_{ref} + \int_{T_{ref}}^{T} C_p \, dT \qquad (J/kg) \qquad \dots (8)$$

Where $h_{ref}$ is the enthalpy at reference temperature $T_{ref}$ and the latent heat term can be written in terms of the latent heat (L) of the material (J/kg).as:
$$L = \Delta H \, \lambda \qquad \dots (9)$$

Where $\Delta H$ may vary from zero for a solid to L for a liquid. Therefore, the liquid fraction, $\lambda$, can be defined as
$$\lambda =$$
$$\begin{cases} \dfrac{\Delta H}{L} = 0 & T < T_m \\[2mm] \dfrac{\Delta H}{L} = \dfrac{T - T_{solidus}}{T_{liquidus} - T_{solidus}} & T_m < T < T_m + \Delta T_m \\[2mm] \dfrac{\Delta H}{L} = 1 & T > T_m + \Delta T_m \end{cases}$$
$$\dots (10)$$

## 2.2. Initial and boundary conditions

Initially at t=0, (solid PCM) at an initial temperature, $T_{initial}$= 299 K. Furthermore, no-slip boundary conditions are considered at the solid-fluid interface. At time t > 0, Reynolds number is to be in the laminar flow regime, Re < 2300, adiabatic boundary condition is applied on all sides of the test section else the lower and upper of the system, as shown in Figure (1).
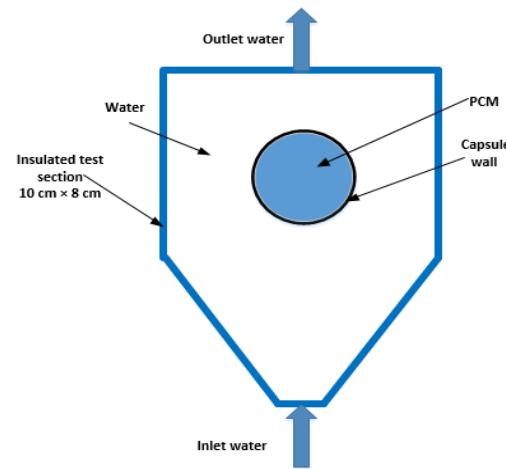


Fig. (1): Numerical model

## 3. NUMERICAL METHOD

A 2D mathematical transient melting thermo-fluid model for PCM is developed by using CFD ANSYS FLUENT 2019R2, where the governing partial differential equations (PDEs) (continuity, momentum and energy) are solved, the semi-implicit (SIMPLE), pressure staggering option (PRESTO), and second-order upwind schemes are used. The time step is carefully chosen to be 0.5 s. At liquid mass fraction (amount of PCM liquid mass) has been updated using equation (10). The mesh size and time intervals are considered after a careful examination of results to achieve grid independency (selected 0.0005 m, 57639 elements), see Figure (2).
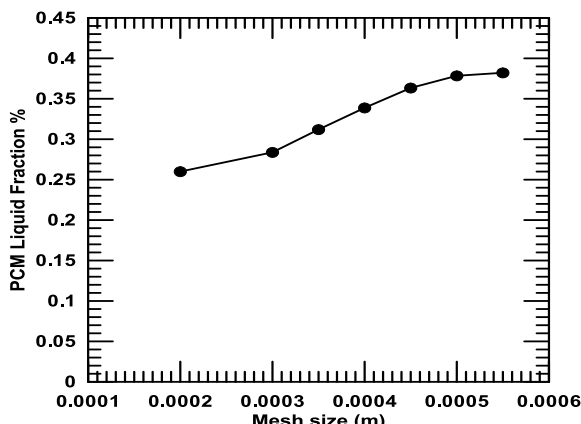
Fig. (2): Relation between lauric acid liquid fraction and mesh size after 10 min of melting for water mean inlet temperature 327.9 K and inlet water mean velocity of 0.0059 m/s (pyrex-glass capsule).

The numerical solution convergence was tested at each time step with the convergence measure of $10^{-6}$ for all results.

In the present work, the following assumptions are employed:
1. Two - dimensional geometries.
2. PCM is a pure substance, so the sub-cooling effect is negligible.
3. Capsulated PCM is placed in a cross flow with the heat transfer fluid.
4. Molten PCM and the heat transfer fluid are considered to be incompressible flow.
5. Physical properties such as viscosity, thermal conductivity, specific heats of solid and molten PCM are constant.

## 4. EXPERIMENTAL TEST RIG
A schematic diagram of the experimental test rig is shown in Figure (3). The test rig is essentially consists of hot water storage tank made of galvanized steel through a set of two valves enabling closed-loop operation. A 30W circulation water pump, head 1.2 m

having a maximum capacity of 22 L/min is also available on the water storage tank which is rectangular in shape (length 30 cm × width 25 cm × height 30 cm). The test section shown in Figure (4) is a rectangular galvanized steel having a dimensions (10 cm × 8 cm) and 0.2 cm thickness. It is insulated with 7.5 cm thick layer of rock wool from three faces else the front face in order to allow direct visualization and photography of the melting process and also to minimize the heat loss from the acrylic sheet transparent face by low thermal conductivity (k=0.17 W/m K). The test section contains one cylindrical pyrex-glass PCM capsule thin walled (0.2 cm) with diameter 2.6 cm, and length 7.6 cm. The cylinder is filled with lauric acid with a mass of 0.04 kg with 99 % purity as shown in Figure (5). Water passes through the chlorinated polyvinyl chloride (CPVC) pipe with rock wool insulation to transfer energy. The cylindrical capsule was then put horizontally into the middle of the rectangular galvanized steel tank, through which hot water entered from the bottom of the test section passing around the capsule. The thermophysical properties of the lauric acid and paraffin wax are given in Table (1), [13] and [14]. The top section of the galvanized steel collectors-storage tank also contains ١٢٠٠ W electrical heater with temperature control in order to enable controlled hot water temperature via a variac (TROIDAC) to control voltage. The measurement system includes a total of six pre-calibrated K-type thermocouples, three of them are distributed horizontally, before the water outlet from the storage tank, while another three were distributed at the water inlet to the storage tank. All thermocouples are connected to a YOKOGAWA 3087 portable hybrid recorder connected to a PC to enable the continuous recording of the temperature readings during various test. Experiment is conducted for Reynolds number of 287 and inlet mean water temperature of 327.9 K.
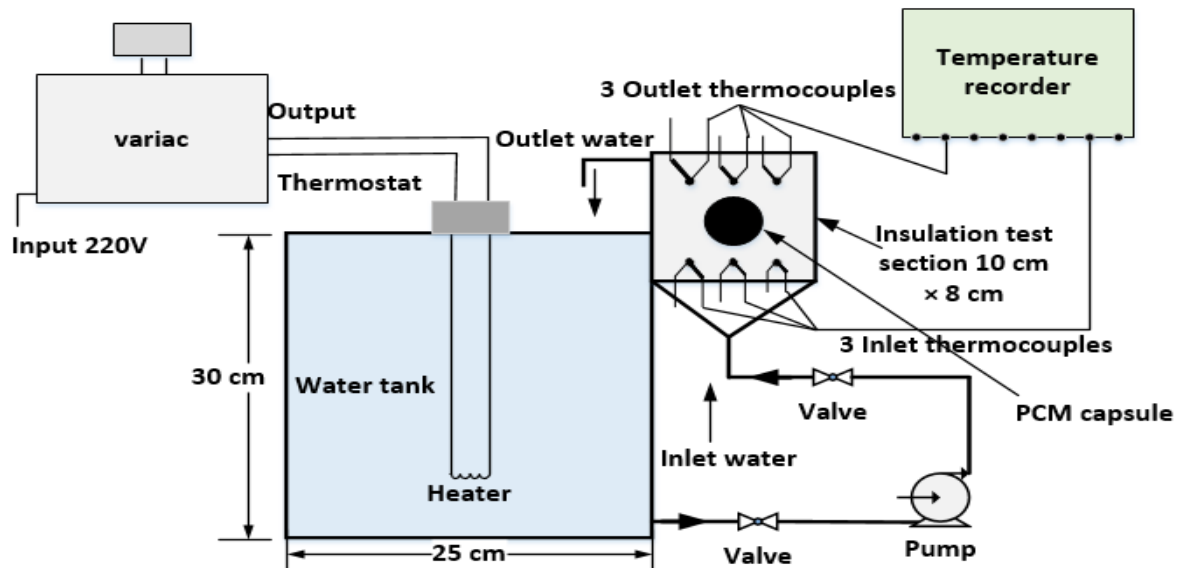
Fig. (3): Experimental test rig block diagram
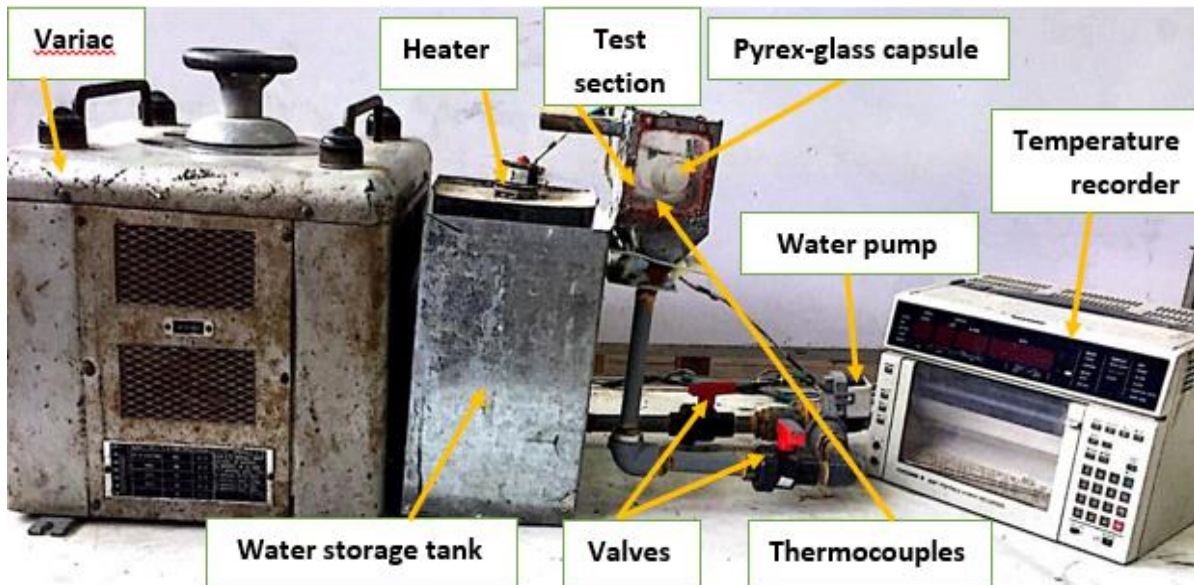

Fig. (4): Photography of the experimental test rig


Fig. (5): The lauric acid capsule photography

Table (1): Thermophysical properties

| Properties | Lauric Acid | | Paraffin Wax | |
|---|---|---|---|---|
| | solid | liquid | solid | liquid |
| Latent Heat of Fusion (J/kg) | 1295·· | | 278800 | |
| Melting Temperature (K) | 313.48 | 315.48 | 327.22 | 329.22 |
| Specific Heat Capacity (J/kg.K) | 2180 | 2390 | 2384 | 2440 |
| Thermal Conductivity (W/m.K) | 0.16 | 0.14 | 0.15 | |
| Dynamic Viscosity (kg/m.s) | 0.0059295 | | 0.0063 | |
| Density (kg/m$^3$) | 940 | 885 | 890 | 712 |
| Thermal Expansion Coefficient (1/K) | 0.00083 | | 0.000714 | |

## 5. MODEL VALIDATION

Numerical simulations were conducted, and the predicted results were compared with the available experimental data in existing studies to validate the developed comprehensive model. The experiments were conducted at combustion laboratory of Mansoura University. The experiments were compared with numerical simulation at inlet HTF temperature of 327.9 K and inlet water mean velocity of 0.0059 m/s for lauric acid. The complete melting time of PCM with a deviation between the experimental and numerical simulation of 2.6 % is shown in Figure (6).

| Theoretical | Experimental | Theoretical | Experimental |
|---|---|---|---|



| Time= 2 min | Time= 6 min |
|---|---|
| Time=10 min | Time= 14 min |
| Time=18 min | Time=22 min |

Time=24.63m in    Time=25.3 min
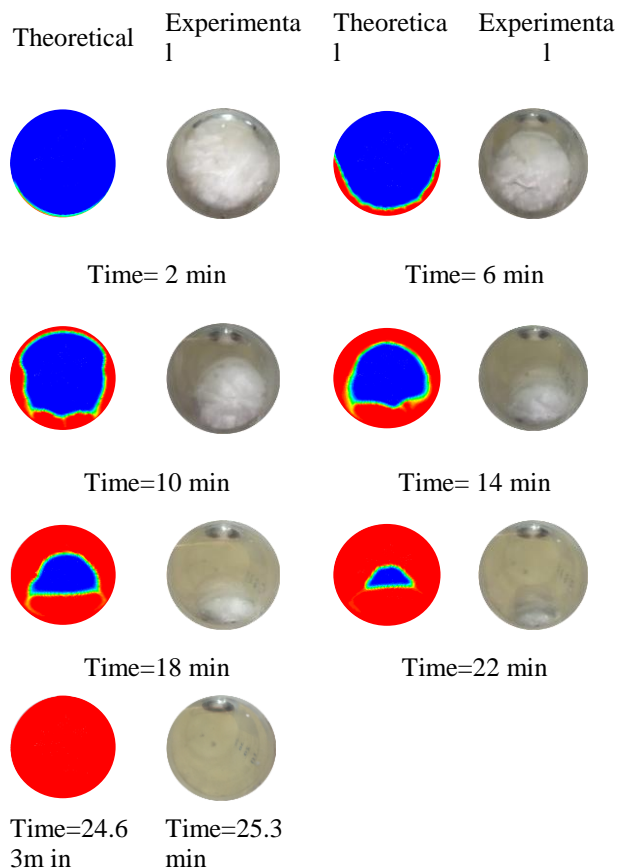
Fig. (6): Comparison between experimental image and theoretical contours for inlet HTF temperature of 327.9 K

## 6. RESULTS AND DISCUSSION

CFD ANSYS 2019R2 dimensional transient heat transfer analysis is conducted for lauric acid and paraffin wax inside cylindrical capsules with pyrex-glass wall.

### 6.1. Effect of inlet HTF temperature

The developed CFD model is used to simulate the PCM charging process at constant HTF flow velocity of 0.0059 m/s at variable inlet temperature of 327.9 K, 333.7 K, 338 K and 343 K and pyrex-glass capsule is used. The selections of these inlet temperatures are all applicable for the actual operation of indirect solar assisted heat pump system where the PCM is integrated. The temporal variations of liquid fraction, PCM temperature, and energy stored at the PCM capsule can thus be simulated at constant fluid flow velocity but different inlet HTF flow temperatures, as shown in Figures (7 to 9).

Figure (7) indicates the relation between lauric acid liquid fraction and time, where the liquid fraction inside the capsule increases with time and HTF temperature.

Figure (8) indicates the relation between lauric acid mean temperature and time, it is shown that the lauric

acid mean temperature increases with time and HTF temperature.

Figure (9) indicates the relation between lauric acid energy stored and time. This figure shows that the energy stored increases with time and HTF temperature. Figure (10) indicates the relation between lauric acid total melting time and inlet water mean temperature, where the total melting time decreases with the increase in the inlet hot water mean temperature.
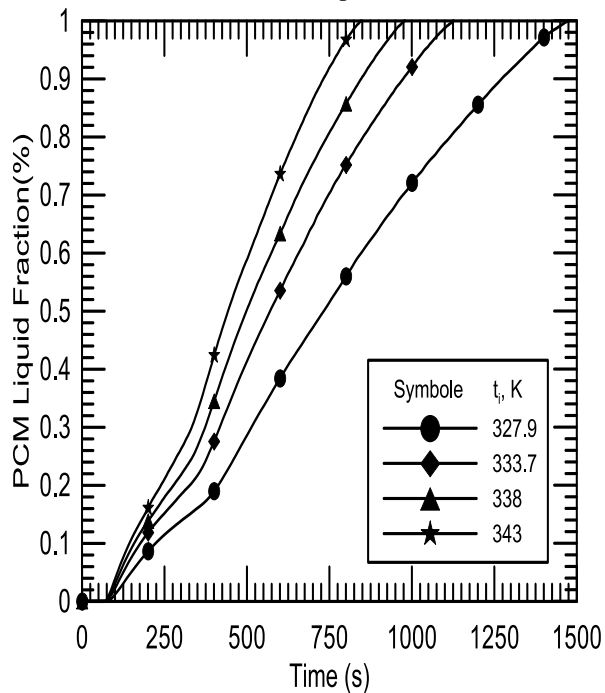


Fig. (7): Relation between lauric acid liquid fraction and time for different water mean inlet temperature and inlet water mean velocity of 0.0059 m/s (pyrex-glass capsule).
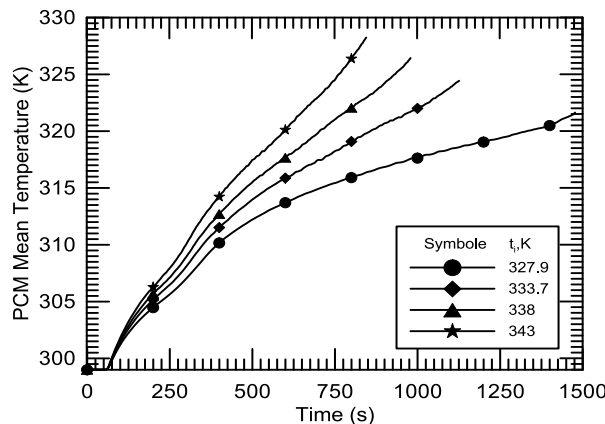


Fig. (8): Relation between lauric acid mean temperature and time for different water mean inlet temperature and inlet water mean velocity of 0.0059 m/s (pyrex-glass capsule)
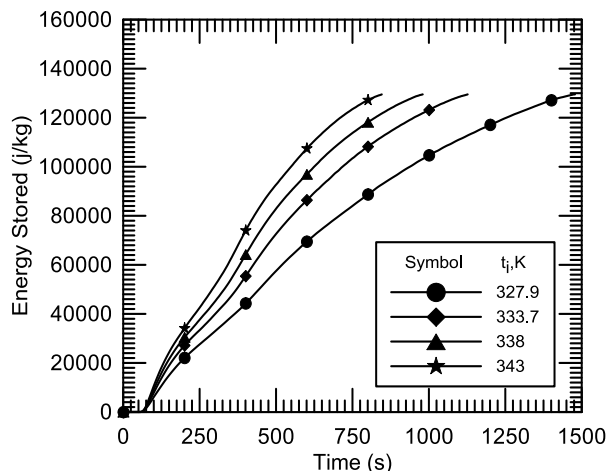


Fig. (9): Relation between lauric acid energy stored and time for different water mean inlet temperatures and an inlet water mean velocity of 0.0059 m/s (pyrex-glass capsule).
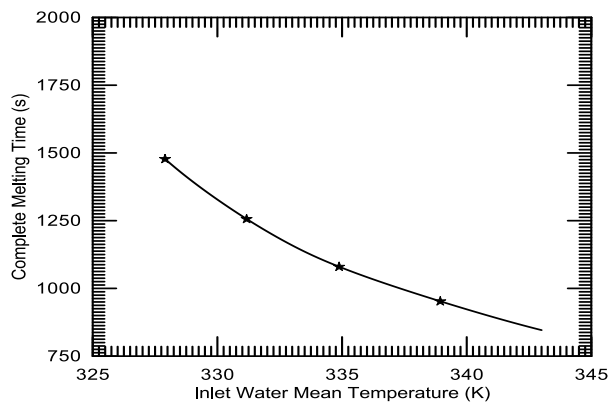


Fig. (10): Relation between lauric acid total melting time and inlet water mean temperature at an inlet water mean velocity 0.0059 m/s (pyrex-glass capsule)

## 6.2. Effect of inlet HTF velocity

Five HTF inlet velocity (0.005, 0.008, 0.011, 0.02, and 0.029) m/s are investigated. The HTF inlet mean temperature equals 327.9 K and pyrex-glass capsule is used.

Figure (11) indicates the relation between lauric acid liquid fraction and time, the figure shows that the liquid fraction of PCM increases with time and inlet velocity of the hot water flow.

Figure (12) indicates the relation between lauric acid mean temperature and time. It is shown that, increasing time, increases the mean temperature of the PCM. Also increases the inlet velocity of the hot water flow increases mean PCM temperature.

Figure (13) indicates the relation between lauric acid energy stored and time. The energy stored in the PCM increases with time and inlet velocity of the hot water flow.

It is clear from Figure (14) that increasing the velocity caused to reduce the total malting time of the PCM in

the pyrex-glass capsule. The increase of the heat transfer fluid velocity can enhanced its overall convection heat transfer and thus speed up the charging process during the phase change period. Since the main thermal resistance is in the PCM side, the thermal resistance reduction on the HTF flow side due to the high velocity has small effect on the overall heat transfer during this period.
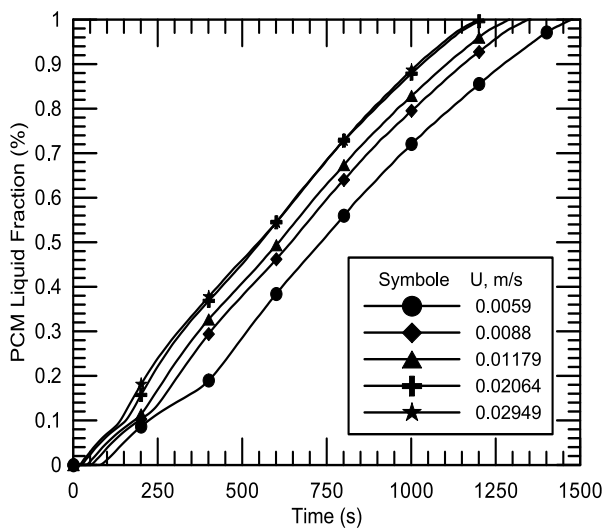


Fig. (11): Relation between lauric acid liquid fraction and time with different water inlet mean velocities for an inlet water mean temperature of 327.9 K (pyrex-glass capsule).
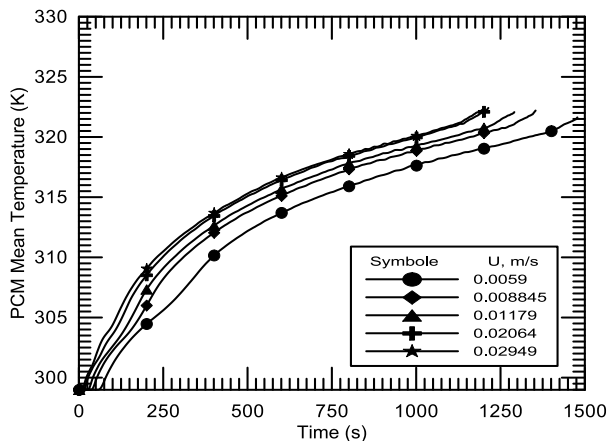


Fig. (12): Relation between lauric acid mean temperature and time for different water inlet mean velocities for an inlet water mean temperature of 327.9 K (pyrex-glass capsule)
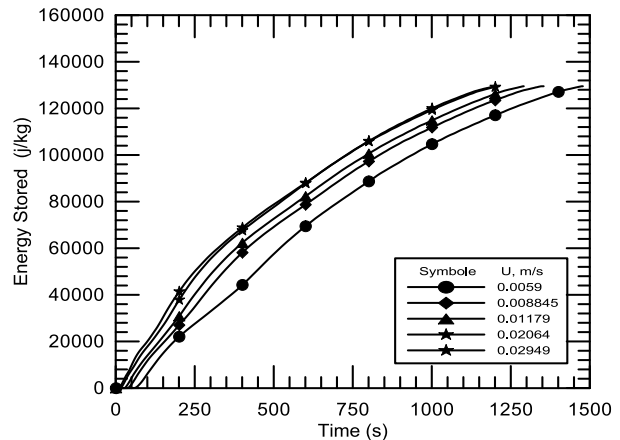


Fig. (13): Relation between lauric acid energy stored and time for different inlet mean velocities for an inlet water mean temperature of 327.9 K (pyrex-glass capsule)
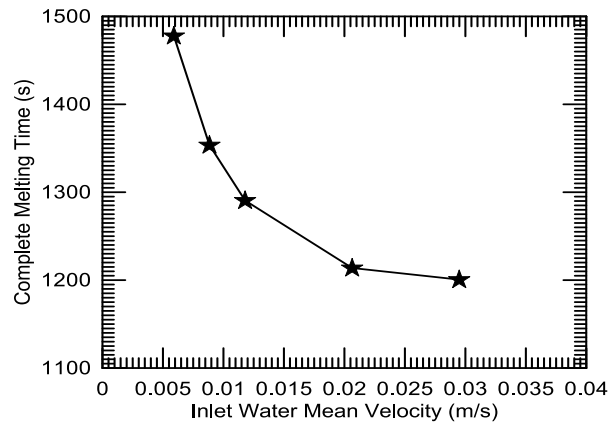


Fig. (14): Relation between lauric acid total melting time and inlet water mean velocity at an inlet water temperature of 327.9 K for (pyrex-glass capsule)

**6.3. Effect of capsule wall conductivity**
CFD model is used to simulate the PCM melting process at constant HTF flow velocity of 0.0059 m/s and water mean inlet temperature of 327.9 K with different thermal conductivities (387.6, 73, 1.1, 0.33) W/m.K for different PCM capsule material (copper, iron, pyrex-glass, and polyethylene) respectively. Figures (15 to 17) show the effect of varying material of capsule wall on the lauric acid liquid fraction, PCM mean temperature, and energy stored.

Figure (15) indicates the relation between lauric acid liquid fraction and time. The liquid fraction of lauric acid inside the PCM capsule increases with time and thermal conductivity.

Figure (16) indicates the relation between lauric acid mean temperature and time. The PCM mean temperature increases with time and thermal conductivity.

Figure (17) indicates the relation between lauric acid energy stored and time for different capsule materials.

It is shown that energy stored in the PCM capsule increases with time and thermal conductivity.

Figure (18) shows the relation between the thermal conductivity of different capsule materials and total melting time for lauric acid. The total melting time in the PCM pyrex-glass capsule decreases with the increase of thermal conductivity.
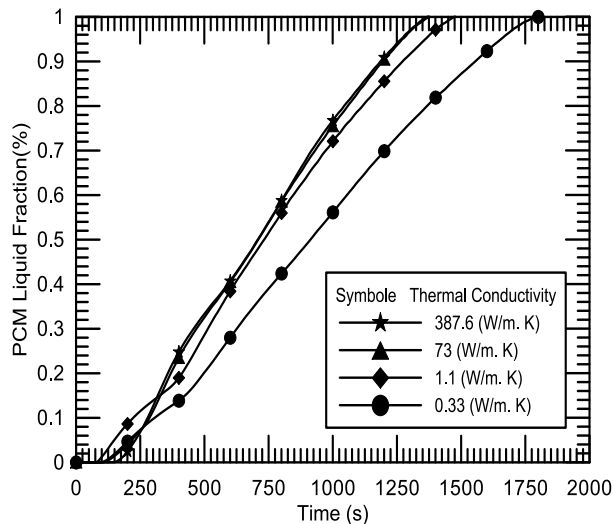


Fig. (15): Relation between lauric acid liquid fraction and time for different thermal conductivities of capsule material wall at water mean inlet temperature 327.9 K and inlet water mean velocity of 0.0059 m/s
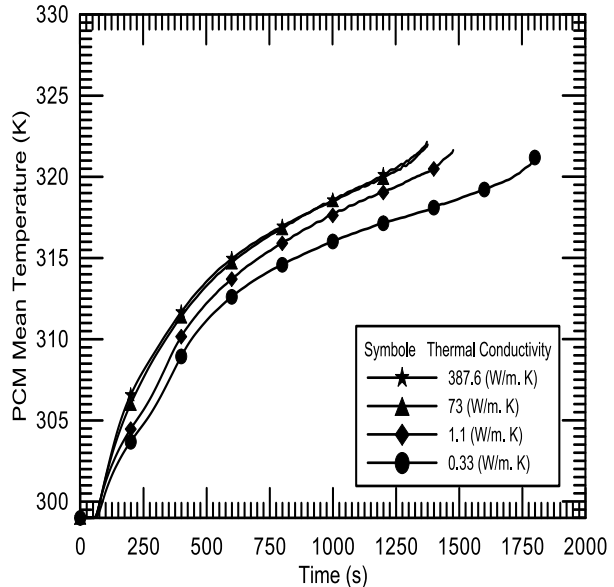


Fig. (16): Relation between lauric acid mean temperature and time for different thermal conductivities of capsule material wall at water mean inlet temperature 327.9 K and inlet water mean velocity of 0.0059 m/s.
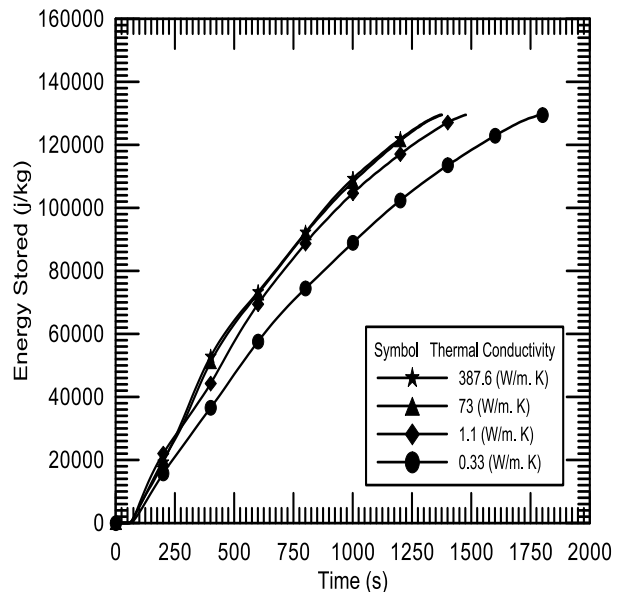


Fig. (17): Relation between lauric acid energy stored and time for different thermal conductivities of capsule material wall at water mean inlet temperature 327.9 K and inlet water mean velocity of 0.0059 m/s.
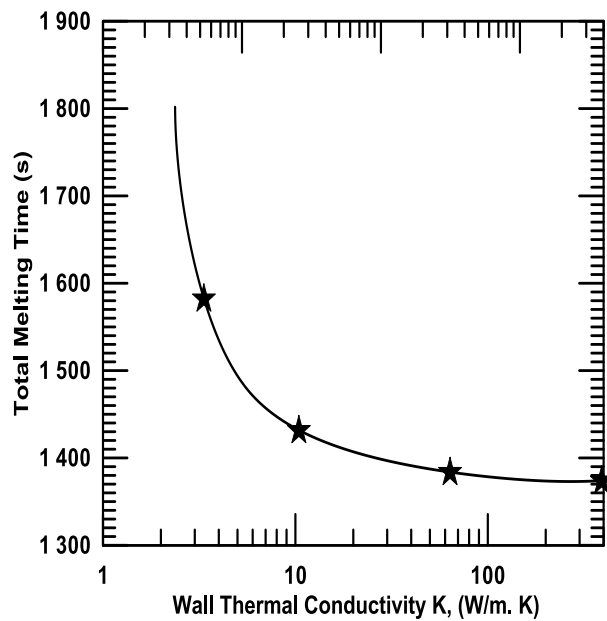


Fig. (18): Relation between thermal conductivity of capsule material wall to total melting time for lauric acid at water inlet mean temperature 327.9 K and inlet mean water velocity 0.0059 m/s.

## 6.4. Comparison between lauric acid and paraffin wax

Figures (19 and 20) show the comparison between the liquid fraction and energy stored with time for lauric acid and paraffin wax as PCMs with inlet mean water temperature of 338 K, inlet mean water velocity 0.0059 m/s, and the same capsule material (pyrex-glass). It is shown from the figures, that the total melting time of

the paraffin is higher than that of lauric acid (approximately 3 times) as shown in Figure (19). The lauric acid energy stored for the same working fluid is lower than paraffin wax as shown in Figure (20) because of the lower lauric acid latent heat of fusion than paraffin wax.

It is clear from the result of the Figures (19-20), that it is possible to give amount of latent heat of fusion from lauric acid (410863 J/kg) during the total melting time of paraffin wax more than paraffin wax (278800 J/kg) by 47%.
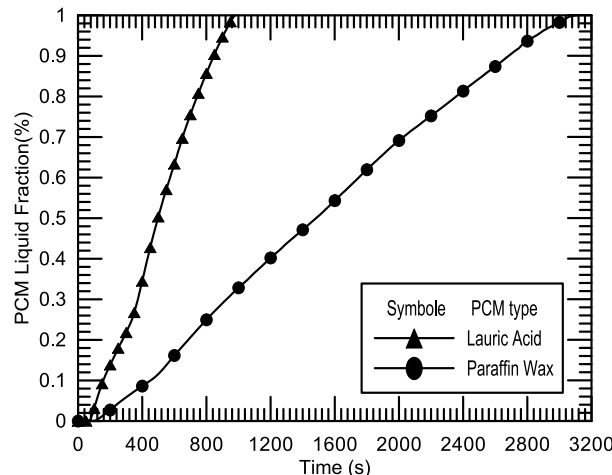


Fig. (19): Relation between liquid fraction for different PCMs for water mean inlet temperature 338 K and an inlet water mean velocity of 0.0059 m/s (pyrex-glass capsule).
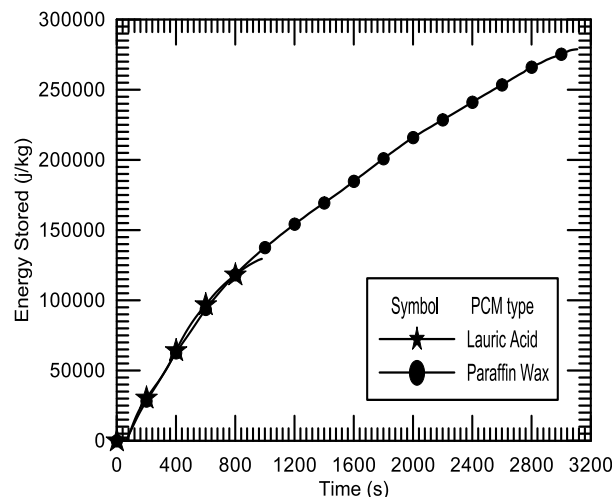


Fig. (20): Relation between energy stored and time for different PCMs to water mean inlet temperature of 338 K and an inlet water mean velocity of 0.0059 m/s (pyrex-glass capsule).

## 7. Conclusions

A numerical and an experimental study of transient laminar flow past cylindrical PCM capsule is presented. The numerical finite-volume method is utilized two-dimensional CFD simulations to study the thermal characteristics of an energy storage system. The effect of the different water mean inlet temperature, different water inlet mean velocity, different capsule material and different PCM is presented. For all examined cases, the following conclusions are made:

1- The lauric acid melting time decreases with the increase of the inlet mean water temperature. The enhancement in the total time melting is 43% for 4.6% increase in water mean inlet temperature.
2- Increasing the inlet water velocity (Reynolds number) decreases the melting time of the lauric acid. The enhancement in the total melting time is 18% for 500% increase in inlet water mean velocity.
3- The melting time decreases with the increase of capsule thermal conductivity. The improvement in the total time melting is 7% when used copper capsule wall.
4- The energy stored of the paraffin wax is higher than that lauric acid for the same working fluid, and capsule size with same material wall, but when compared to the total melting time of paraffin wax to lauric acid, which is approximately three times the melting time of lauric acid, the amount of latent heat stored to the lauric acid pyrex-glass capsule is 47% higher than paraffin wax capsule if the lauric acid is melted at the same time as paraffin wax.

## REFERENCES

[1]    H. A. Adine and H. El Qarnia, "Numerical analysis of the thermal behaviour of a shell-and-tube heat storage unit using phase change materials," Appl. Math. Model., vol. 33, no. 4, pp. 2132–2144, 2009.
[2]    W. Zhao, "Characterization of Encapsulated Phase Change Materials for Thermal Energy Storage," p. 113. [Doctor of Philosophy], Mechanical Engineering Department Lehigh University. 2013.
[3]    M. Hlimi et al., "Melting inside a horizontal cylindrical capsule," Case Stud. Therm. Eng., vol. 8, no. September, pp. 359–369, 2016.
[4]    S. Blancher et al., "A numerical analysis of solid – liquid phase change heat transfer A numerical analysis of solid – liquid phase change heat transfer around a horizontal cylinder," Appl. Math. Model., vol. 38, no. 3, pp. 1101–1110, 2015.

[5]     A. K. Alshara,. "Numerical Investigation of Energy Storage in Packed Bed of Cylindrical Capsules of PCM. Engineering and Technology Journal Volume: 32 Issue: 2 Part (A) EngineeringPages:494-510, 2016.

[6]     Tan, F. L., S. F. Hosseinizadeh, J. M. Khodadadi, and Liwu Fan. "Experimental and Computational Study of Constrained Melting of Phase Change Materials ( PCM ) inside a Spherical Capsule." International Journal of Heat and Mass Transfer 52:3464–72, 2009.

[7]     S. Karthikeyan and R. Velraj, "Numerical investigation of packed bed storage unit filled with PCM encapsulated spherical containers - A comparison between various mathematical models," International Journal of Thermal Sciences., vol. 60, pp. 153–160, 2012.

[8]     S. Tripathi and A. Tomar, "CFD Analysis and Melting Performance of PCMs in two dimensional sphere," International Research Journal of Engineering and Technology(IRJET) Volume: 04 Issue: 07 page: 3350-3358, 2017.

[9]     W. Xiong, A. Banerjee, and G. Harlow, "Numerical and Experimental Study of the Melting Process of a Phase Change Material in a Partically Filled Spherical Shell," Lehigh University Lehigh Preserve Theses and Dissertations, 2017.

[10]    L. Yang, X. Zhang, and G. Xu, "Thermal performance of a solar storage packed bed using spherical capsules filled with PCM having different melting points," Energy and Buildings., vol. 68, no. PART B, pp. 639–646, 2014.

[11]    M. Emam and M. Ahmed, "Cooling concentrator photovoltaic systems using various configurations of phase-change material heat sinks," Energy Convers. Manag., vol. 158, no. January, pp. 298–314, 2018.

[12]    K. Kant, A. Shukla, A. Sharma, and P. Henry, "Heat transfer studies of photovoltaic panel coupled with phase change material," Solar Energy, vol. 140, pp. 151–161, 2016.

[13]    B. Kamkari and H. Shokouhmand, "Experimental investigation of phase change material melting in rectangular enclosures with horizontal partial fins," International Journal of Heat and Mass Transfer vol. 78, pp. 839–851, 2014.

[14]    M.Thirugnanam.C,"Experimental Analysis of Latent Heat Thermal Energy Storage using Paraffin Wax as Phase Change Material." International Journal of Engineering and Innovative Technology (IJEIT) 3(2):372–76, 2013.